Journal of Thermal Engineering
Web page info: https://jten.yildiz.edu.tr
DOI: 10.18186/thermal.977975

Research Article

Parametric investigation of open-drive scroll expander for micro organic rankine cycle applications

Suhas UPADHYAYA[1,*], Veershetty GUMTAPURE[1]

[1]Department of Mechanical Engineering, National Institute of Technology Karnataka, Surathkal, Mangalore, India

ARTICLE INFO

Article history
Received: 7 August 2019
Accepted: 3 November 2019

Key words:
Organic rankine cycle; Scroll expander; Expansion ratio; Semi-empirical model

ABSTRACT

Organic Rankine cycles (ORC) are used to produce power from low-temperature heat sources. In the low power output range (<10 kW_e), scroll expanders are preferred. However, the performance of the ORC system is dependent on the expander efficiency. The present work focuses on the parametric investigation of the open-drive scroll expander used for micro-organic Rankine cycle. A 5 kW_e expander was used and its built-in volume ratio was 3.5. R245fa was used as the working fluid. The analysis was carried out using a well-known semi-empirical model available in the literature. Effect of key parameters such as expansion ratio, shaft speed, and expander inlet temperature on power output and expander efficiency wasevaluated for four different cases. Results showed that, at an inlet pressure of 10 bar, peak efficiency of 58% and 60% was achieved at shaft speeds of 1500 RPM and 2000 RPM respectively. It was also evident that,at higher shaft speeds, the increase in mass flow rate is not sufficient to counter frictional and mechanical losses within the expander. The analysis also indicated that increasing the expander inlet temperature could have a negative impact on the expander efficiency as well as the overall performance of the ORC system, as the thermal energy dissipation is higher at higher inlet temperatures for all cases.

Cite this article as: Upadhyaya S, Gumtapure V. Parametric investigation of open-drive scroll expander for micro organic rankine cycle applications. J Ther Eng 2021;7(5):1110–1120.

INTRODUCTION

Climate change and global warming have become a major concern for the world. The global community has committed itself to increase energy sustainability by increasing renewable energy generation and reducing dependency on fossil fuels. To counter the effects of climate change, India has committed to increasingits renewable energy share to 40% by 2030 at the COP21 climate summit in Paris [1]. With rapid industrialisation and urbanisation, achieving this target is an uphill task. India has grown by leaps and

*Corresponding author.
*E-mail address: suhas.upa@gmail.com, veersg@yahoo.co.in

This paper was recommended for publication in revised form by Regional Editor Mehdi Bahiraei

Published by Yıldız Technical University Press, İstanbul, Turkey

bounds as far as Solar PV and wind energy is concerned. However, it is not enough to achieve the targets set by the Govt. of India. One of the technologies which have received much attention over the recent years is organic Rankine cycle (ORC) technology. Low-grade heat with temperatures ranging from 60 to 200 °C can be effectively utilised using ORC. This heat can be extracted by various means such as Solar [2, 3, 4], waste heat recovery [5–11], biomass [12], geothermal [13, 14], etc. Heat is absorbed by the organic fluid with a low boiling point, in the evaporator. The high-pressure vapour is then passed through the expander which produces power. ORC technology is preferred over other conventional power generating systems because of its low operating pressures, compactness andsimplicity, ease of operation, and low maintenance. However, the irreversibilities associated with each of the components in ORC have to be minimised. The most important component in ORC is the expansion device or the turbine which converts the available thermal energy into mechanical work. Scroll expander operates at low rotational speeds, higher pressure ratios, and costs less compared to dynamic machines and screw expanders. Therefore, scroll expanders are known to be the most appropriate expansion device for micro ORC applications (1–10 kW_e). Sincesmall-scale expanders are not readily available in the market, researchers have found a novel method of using commercially available scroll compressors and modifying themin such a way that it works as an expander [15–18]. However, the expansion volume ratio need not necessarily match with the built-in volume ratio of the expander as it is not designed for that particular application. In the recent past, many experimental studies have been conducted to demonstrate the use of scroll expanders as an expansion devices for micro ORC power generation systems. Chang et al. [19] analysed a modified scroll expander and they observed that the expander efficiency and cycle efficiency increased with an increase in superheating. Declaye et al. [20] conducted experimental studies of an open drive scroll expander modified from a commercially available air compressor, using R245fa as the working fluid. They obtained maximum isentropic efficiency of 75.7% and maximum shaft power of 2.1 kW. They also concluded that oil-free expanders have an advantage over hermetic expanders because of theirsimplistic design and ease of operation. Qiu et al. [21] examined the performance of a modified scroll expander driven by compressed air. They observed that the power output of the expander increased significantly with an increase in shaft speed.

In the recent past, few works havebeen published related to performance characterisation of scroll expanders and optimisation of their geometry and operating conditions. For instance, researchers developed mechanistic models which predict the internal behaviour of the machine based on their geometry and configuration [22, 23]. But the drawbacks of these models has been that it requires a number of sub-models such as valve model, internal leakage model, motion equation, heat transfer equation, etc. to account for internal leakages, heat transfer surface, and other mechanical losses. Hence, it becomes more complicated and cannot be integrated into cycle models. In general, low-order mathematical models are preferred for thermal systems [24–39]. However, in the case of scroll expanders for small-scale power generation, empirical and semi-empirical models are preferred for performing cycle analysis.

Manyexperimental and theoretical studies have been carried out on the performance characterisation of scroll expanders. A few of them have been tabulated in Table 1. However, limited efforts have been made to analysethe key operating parameters of the expander and its effect on the expander performance. It is important to carry out a parametric study to analyse the off-design performance of the scroll expander with respect to its efficiency and work output. This paper aims to investigate the performance of the scroll expander under varying operating conditions, using a validated semi-empirical model available in the literature [40]. Using this model, the effect of expansion ratio, shaft speed, and expander inlet temperature on the mass flow rate, work output, and expander efficiency havebeen analysed. The expander capacity was 5 kW, the built-in-volume ratio was 3.5 and the maximum permissible pressure was 13.5 bar. R245fa was used as the working fluid. Rotational speeds couldbe varied from 500 RPM to 3600 RPM.

MODEL DESCRIPTION

Thesemi-empirical model describes the expansion process within the scroll expander which also consists of related equations. The entire expansion process is divided into 7 stages as shown in fig. 1. The processes are as follows:

a) Adiabatic supply pressure drop (su to su,1)
b) Constant pressure supply cooling down (su,1 to su,2)
c) Internal leakage (su,2 to ex,2)
d) Adiabatic and reversible expansion to the adapted pressure which is forced upon by the built-in volume ratio of the machine (su,2 to ad)
e) Adiabatic expansion at constant volume (ad to ex,2)
f) Adiabatic fluid mixing between supply and leakage flows (ex,2 to ex,1)
g) Constant pressure exhaust heat transfer (ex,1 to ex)

Following assumptions were used to simplify the analysis:

1) Adiabatic supply pressure drop is modelled as isentropic flow through a converging nozzle whose cross-sectional area is A_{su}. A_{su} represents the average inlet port effective area during the suction process.
2) Supply and exhaust heat transfer is simulated using a fictitious envelope with uniform temperature T_w. This envelope represents the outer shell of the expander and the scrolls. Heat transfer occurs between the supply chamber and this envelope.

Table 1. Recent studies on scroll expanders for micro organic Rankine cycle application

Reference	Type of study & operating conditions	Remarks
Vincent et al. [44]	Type: Experimental Working fluid used: R245fa N = 2660 RPM Expansion ratio: 5.7 Evaporation temperature: 140°C Evaporation pressure: 6–16 bar	Maximum work output : 2.2 kW_e Maximum expander efficiency: 68%
Wang et al. [45]	Type: Experimental Working fluid used: R134a N = 3670 RPM Expansion ratio: 2.65–4.84 Evaporation pressure: 8–9 bar	Maximum work output : 0.8 kW_e Maximum expander efficiency: 77%
Davide et al. [40]	Type: Experimental and performance characterisation using semi-empirical model. Working fluid used: R245fa Evaporation temperature: 110°C N = 1600 RPM	1) Maximum expander efficiency: 58% 2) Model showed good agreement with the experimental data. 3) The model showed that the mechanical losses accounted for up to 19% of the shaft power at 3000 RPM.
Jingye et al. [41]	Type: Experimental validation of scroll expander semi-empirical model Working fluid used: R1223zd(E) and R245fa	Maximum deviation between measured and predicted results of supply pressure, exhaust temperature and net power output are 3.35%, 2.24 K and 6.09%, respectively.
Vincent et al. [42]	Type: Performance characterisation of scroll expander using a semi-empirical model and its validation. Working fluid used: R123	Maximum deviation between measured and predicted results is 2% for mass flow rate, 5% for shaft power and 3K for discharge temperature.

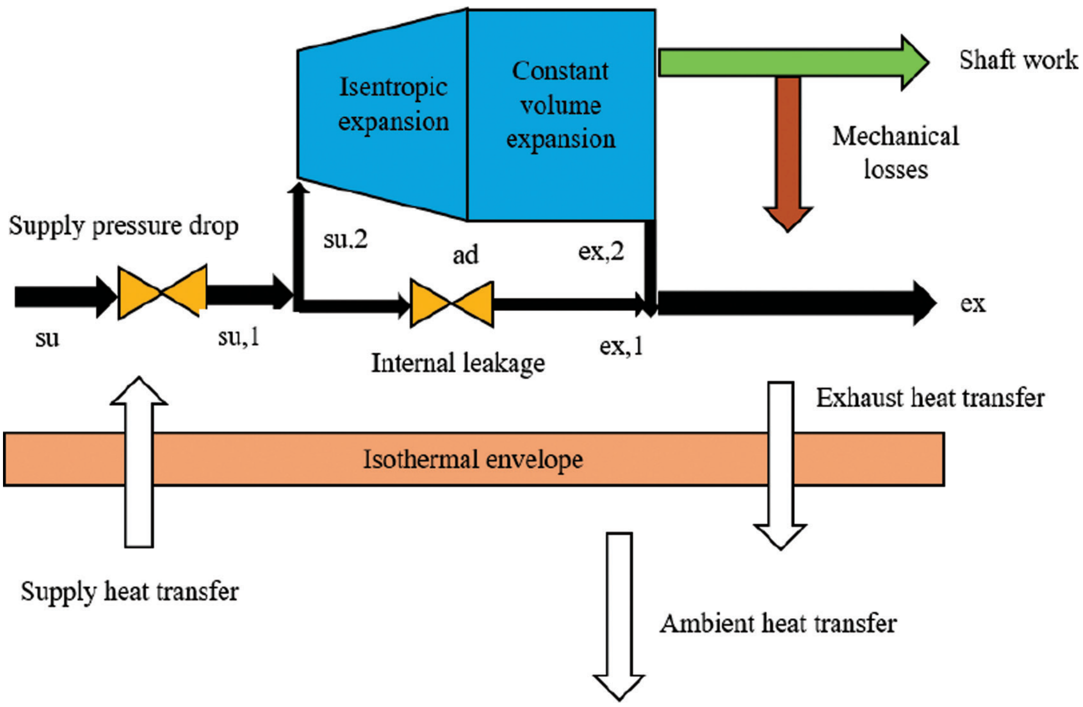

Figure 1. Conceptual diagram of scroll expander mode.

3) Internal leakage is modelled as a lumped nozzle whose cross-sectional area is A_{leak}.
4) There is no pressure drop through the discharge port. Therefore, the model assumes that some fluid flows out of or into the expander chamber (under/over-expansion) instantaneously after the chamber opens to the outlet line.
5) Mechanical losses within the expander are lumped into a constant parameter called τ_{loss}.

Adiabatic Supply Pressure Drop (su to su,1)

This process accounts for the pressure losses occurring between the inlet of the expander and the suction chamber. The pressure drop occurs mainly due to two reasons. The primary reason is that, during the suction process, the expander suction port is blocked by the tip of the orbiting scroll which reduces the effective suction port area. In addition to this, the flow passage is progressively reduced between the chamber and along the length of the scroll.

This process is modelled as isentropic flow through a converging nozzle whose cross-sectional area is A_{su}. A_{su} represents the average inlet port effective area during the suction process. The mass flow rate of the fluid entering the expander can be expressed as [41],

$$\dot{m} = \rho_{su,1} \times A_{su} \times \sqrt{2 \times \left(h_{su} - h_{su,1}\right)} \tag{1}$$

Isobaric Supply Cooling Down (su,1 to su,2)

Supply heat transfer is simulated using a fictitious envelope with uniform temperature T_w. This envelope represents the outer shell of the expander and the scrolls. Heat transfer occurs between the supply chamber and this envelope. This can be modelled as,

$$\dot{Q}_{su} = \dot{m} \times \left(h_{su,1} - h_{su,2}\right) \tag{2}$$

Internal heat transfers are lumped into equivalent supply and exhaust heat transfer rates between the working fluid and a fictitious metal envelope which is maintained at a constant wall temperature T_w. This envelope represents the mass associated with the expander shell, fixed and the orbiting scrolls. The supply heat transfer coefficient AU_{su} varies with the mass flow rate and only the convective heat transfer coefficient of the working fluid is considered. The conductive thermal resistance of the scroll wraps is neglected due to the high metal thermal conductivity and small thicknesses (Lumped system analysis). Therefore, equation 2 can be rewritten as,

$$\dot{Q}_{su} = \left[1 - e^{\frac{-AU_{su}}{\dot{m}C_p}}\right] \times \dot{m} \times C_p \times \left(T_{su,1} - T_w\right) \tag{3}$$

The relationship between supply heat transfer coefficient, AU_{su} and mass flow rate is defined by,

$$AU_{su} = AU_{su,nom} \times \left(\frac{\dot{m}}{\dot{m}_{nom}}\right)^{0.8} \tag{4}$$

where, $AU_{su,nom}$ is the nominal supply heat transfer coefficient corresponding to the nominal mass flow rate. [35]

Internal Leakage (su,2 to ex,2)

Internal leakage is an irreversible loss thatoccurs along two paths in a scroll machine. The first leakage path occurs in the axial clearance between the scrolls and the bottom. This results in radial leakage. The second path is the clearance between the fixed and the orbiting scroll, which leads to tangential leakage. This internal leakage is modelled similar to the supply pressure drop. It is modelled as a lumped nozzle whose cross-sectional area is A_{leak}. Critical pressure of the lumped nozzle is defined as [42],

$$P_{cr} = P_{su,2} \times \left(\left(\frac{2}{\gamma + 1}\right)^{\frac{\gamma}{\gamma - 1}}\right) \tag{5}$$

$$P_{thr} = Max\left(P_{ex,2}, P_{cr}\right) \tag{6}$$

The critical pressure is evaluated by considering the working fluid as a perfect gas. γ indicates the ratio of specific heats C_p and C_v.

The mass flow rate entering the expander is divided into two parts. The first facilitates the rotation of the shaft at a particular speed, N. The second part is the leakage mass flow rate.

Total mass flow rate is given by,

$$\dot{m} = \rho_{su,2} \times \left(\frac{N \times v_s}{r_{v,in}}\right) + \dot{m}_{leak} \tag{7}$$

where, v_s is the swept volume and $r_{v,in}$ is built-in volume ratio of the expander.

Leakage mass flow rate is calculated as,

$$\dot{m}_{leak} = \rho_{leak} \times A_{leak} \times \sqrt{2 \times \left(h_{su,2} - h_{leak}\right)} \tag{8}$$

Adiabatic and Reversible Expansion to the Adapted Pressure (su,2 to ad)

After the initial cooling down, the working fluid undergoes isentropic expansion. The pressure is reduced from $P_{su,2}$ to P_{ad}. This adapted pressure is decided by the built-in volume ratio, $r_{v,in}$ of the expander. This is a geometric parameter of the scroll expander which is designed and fixed by the manufacturers.

$$v_{ad} = r_{v,in} \times v_{su,2} \tag{9}$$

Adiabatic Expansion at Constant Volume (ad to ex,2)

Most of the scroll expanders that are used in organic Rankine cycle systems are modified from a commercially available scroll compressor. The operating pressure of the ORC system does not necessarily match that of the built-in volume ratio of the expander. This leads to under or over-expansion losses. Under expansion occurs when the adapted pressure, P_{ad} exceeds the exhaust pressure, $P_{ex,2}$. The model assumes there is no pressure drop through the discharge port. Hence, in order to equalize the pressures in the exhaust chamber and the discharge line, the model assumes that some fluid flows out of or into the expander chamber (under/over-expansion) instantaneously after the chamber opens to the outlet line.

Adiabatic Fluid Mixing between Supply and Leakage Flows (ex,2 to ex,1)

The mass flow rate responsible for shaft rotation and leakage mass flow rate mix together. This results in the increase in the specific enthalpy of the working fluid ($h_{ex,1} > h_{ex,2}$).

Constant Pressure Exhaust Heat Transfer (ex,1 to ex)

Isobaric exhaust heat transfer is modelled similar to isobaric supply cooling down. Heat is exchanged between the fluid leaving the expander and the metal envelope.

Performance Indicators

Internal expansion work can be calculated as [43],

$$\dot{W}_{int} = \dot{m}_{int} \times \left[\left(h_{su,2} - h_{ad} \right) - v_{ad} \left(P_{ad} - P_{ex,2} \right) \right] \tag{10}$$

Net power output or shaft power is the difference between the internal expansion work and the mechanical losses associated with the expander. In this case, all mechanical losses are lumped into a constant parameter called τ_{loss}.

$$\dot{W}_{sh} = \dot{W}_{int} - \dot{W}_{loss} \tag{11}$$

$$\dot{W}_{loss} = \frac{2 \times \pi \times N \times \tau_{loss}}{60} \tag{12}$$

Expander isentropic effectiveness or expander efficiency is defined as the ratio of net output power to isentropic expansion power [43].

$$\epsilon_{is} = \frac{\dot{W}_{sh}}{\dot{m} \times \left(h_{su} - h_{is} \right)} \tag{13}$$

Thermal losses towards the ambient are evaluated as,

$$\dot{Q}_{amb} = AU_{amb} \times \left(T_w - T_{amb} \right) \tag{14}$$

where, AU_{amb} is the global heat transfer coefficient between the envelope and the ambient [42].

The metal wall temperature is calculated by applying the global heat balance equation which is given by,

$$\dot{W}_{loss} - \dot{Q}_{ex} + \dot{Q}_{su} - \dot{Q}_{amb} = 0 \tag{15}$$

The inputs to the semi empirical scroll expander are listed in table 2. [40]

PARAMETRIC ANALYSIS

Using the semi-empirical model, this study is carried out to examine a single parameter by varying it, while keeping the other parameters constant. The monitored parameters are the expansion ratio, the rotational speed of the shaft, and the inlet temperature of the expander. The outputs to be assessed are mainly mass flow rate, the work output, and the efficiency of the expander.

Effect of Expansion Ratio

Two inlet pressures of 10 bar and 14 bar are considered. The inlet temperature is fixed at 110°C. The expansion ratio is varied by varying the condensation pressure from 3 bar to 1.2 bar. The shaft power and expander efficiency are evaluated for different expansion ratios. The simulation is carried out for rotational speeds of 1500 RPM and 2000 RPM.

It is seen from fig. 3 that the shaft power increases with decreasing condensation pressure or increasing expansion ratio. However, the power curve is shifted downwards at lower shaft speeds at the same inlet pressures. This is due to the decrease in mass flow rate of the working fluid as shown in fig. 2. In addition to this, the two cases with inlet

Table 2. Inputs to the semi empirical model

Parameter	Value	Unit
$\dot{m}_{nom}$	0.1384	kg/s
$AU_{su,nom}$	28.39	W/K
$AU_{ex,nom}$	11.71	W/K
AU_{amb}	6.17	W/K
V_s	8.1×10^{-5}	m^3
$r_{v,in}$	3.31	–
A_{su}	4.01×10^{-5}	m^2
A_{leak}	7.43×10^{-6}	m^2
τ_{loss}	2.97	N-m

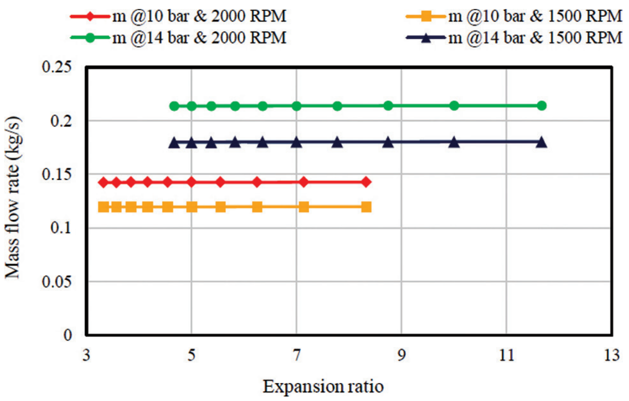

Figure 2. Effect of expansion ratio on mass flow rate of the working fluid.

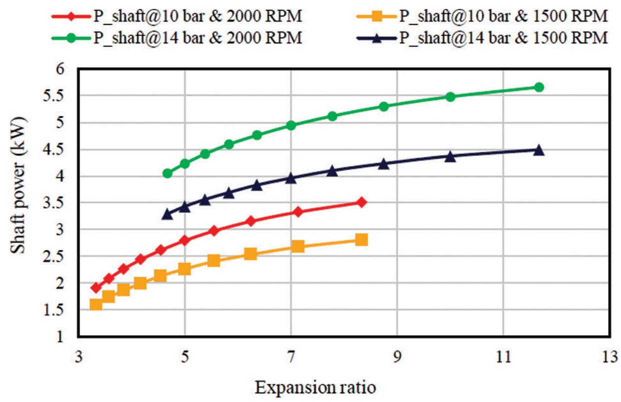

Figure 3. Effect of expansion ratio on shaft power.

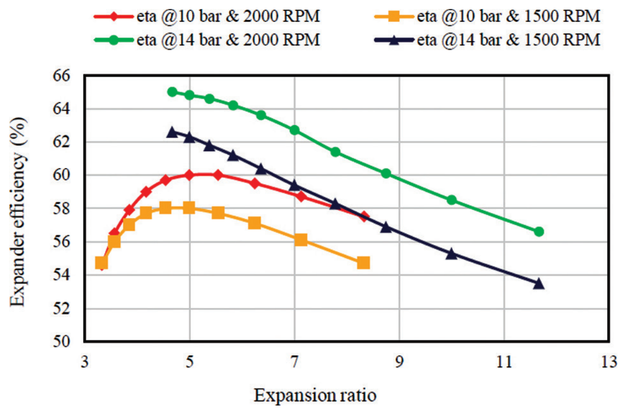

Figure 4. Effect of expansion ratio on expander efficiency.

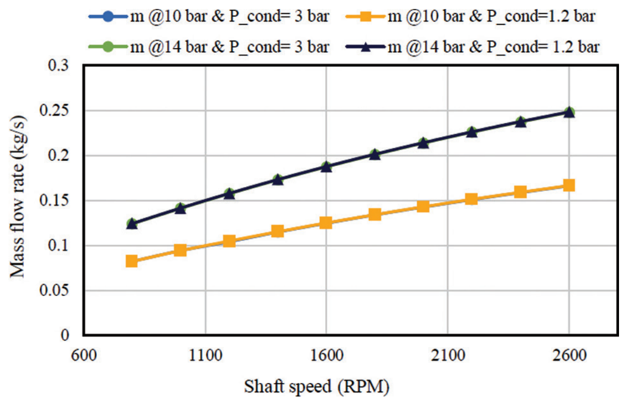

Figure 5. Effect of shaft speed on mass flow rate of the working fluid.

pressure at 10 bar havea lower mass flow rate compared to the two cases with 14 bar inlet pressure. This is because, at higher pressure, the fluid density is also high. Change of expansion ratio means a change in condensation pressure. The mass flow rate of the working fluid is independent of condensation pressure. Hence, there is no change in mass flow rate when the expansion ratio increases.When the inlet pressure is lowered to 10 bar, the power curve shifts downwards and towards the left, with respect to the cases with increased expansion ratios. Extraction of work from the expander also increases at higher expansion ratios which leads to higher power output.

Fig. 4 shows the variation of expander efficiency with expansion ratio. Theexpansion process is divided into two parts. The initial part is the isentropic expansion till the adapted pressure and the second part is the constant volume expansion. In the first part, the pressure of the working fluid is reduced from $P_{su,2}$, to a pressure of adaptation P_{ad} imposed by the built-in Volume ratio of the expander. The built-in volume ratio is an intrinsic geometric parameter of the scroll expander. Under-expansion occurs when the internal pressure ratio imposed by the expander ($P_{su,2}/P_{ad}$) is lower than the system pressure ratio ($P_{su,2}/P_{ex,2}$). In cases when the inlet pressure is fixed at 14 bar and the expansion ratio is varied from 4.67 to 11.67, all condensation pressures (3 to 1.2 bar) leads to the condition of under expansion. The expander efficiency drops when under expansion takes place. The efficiency decreases by 12.92% for shaft speed of 2000 RPM and 14.53% for shaft speed of 1500 RPM.At inlet pressure of 10 bar, a peak is observed inefficiency curve for an expansion ratio of 4.55 and 5 at shaft speeds of 1500 & 2000 RPM, respectively. This is due to the fact that the condensation pressures pass through the adapted condition of the expander, where the efficiency is maximum.

Effect of Shaft Speed

Four different combinations (Inlet pressure at 10 bar and condensation pressure of 3 bar; Inlet pressure at 10 bar and condensation pressure of 1.2 bar; Inlet pressure at 14 bar and condensation pressure of 3 bar; Inlet pressure at 14 bar and condensation pressure of 1.2 bar) are used to study

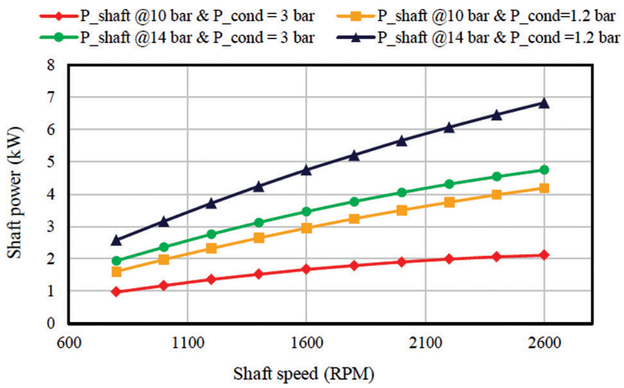

Figure 6. Effect of shaft speed on shaft power.

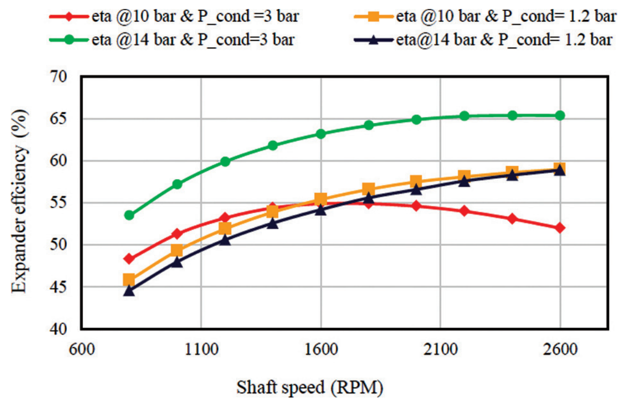

Figure 7. Effect of shaft speed on expander efficiency.

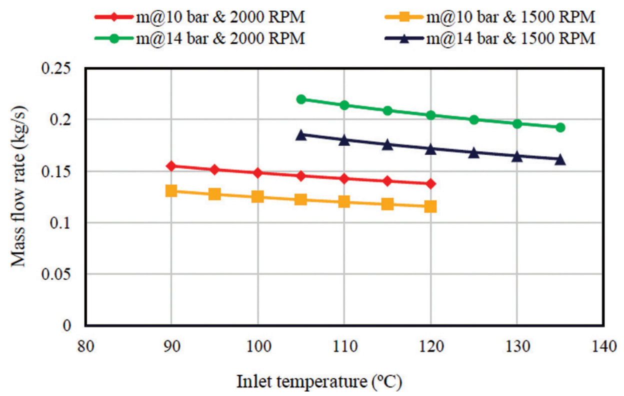

Figure 8. Effect of inlet temperature on mass flow rate.

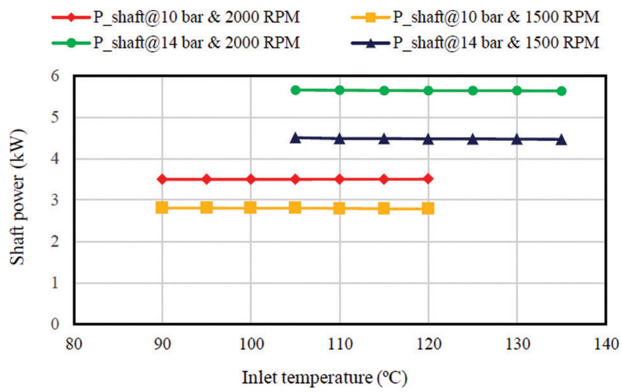

Figure 9. Effect of inlet temperature on shaft power.

the effect of shaft speed on mass flow rate, work output, and expander efficiency. The inlet temperature is fixed at 110°C. The shaft speed is varied from 800 RPM to 2600 RPM.

Fig. 5 shows the variation of the mass flow rate of the fluid with shaft speed. The variation is almost linear with respect to shaft speed. Theoretically higher expansion ratio should lead to increasingin leakage mass flow rate. However, the vapour is already in the choked condition in the case of the lowest expansion ratio (inlet pressure of 10 bar and condensation pressure of 3 bar). Therefore, the curves are superimposed. It is observed that the shaft power crosses a peak value when the shaft speed is varied as shown in fig. 6. Beyond a certain point, the increase in mass flow rate due to increasing shaft speed is not enough to counter the losses occurring within the expander. Mechanical losses occur mainly within the scroll expander due to friction between the fixed and orbiting scroll. However, in this model, all losses are lumped into one mechanical loss torque, .

The effect of increasing speed beyond a certain point can be seen in fig. 7 as the expander efficiency witnesses a marginal drop. The trend is similar for all curves. But, the expander efficiency curve for the inlet pressure of 10 bar and condensation pressure of 3 bar shows that the curve peaks (54.9%) at a shaft speed of 1600 RPM. In other cases, the peak has shifted towards the extreme right (close to 2600 RPM). Power output is reduced due to an increase in losses. Therefore, the expander efficiency decreases. However, the peaks of shaft power and expander efficiency are not the same.

The wall temperature increases as the shaft speed are-increased. This means that the fluid temperature at su,2 was higher. Therefore, the enthalpy at this state, where expander work actually starts, is also high. The mass flow rate of the fluid also increases with an increase in shaft speed. However, the increase in wall temperature also leads to an increase in heat losses and expander outlet temperature. The increase in fluid temperature at the expander outlet assigns heavier heat duty to the condenser which will have a weight on the overall efficiency of the cycle. Hence, the wall temperature plays a major role as far as the power loss is concerned.

Effect of Inlet Temperature

In this case, the fixed parameters are the expander inlet pressures of 10 and 14 bar, condensation pressure of 1.2 bar, and shaft speeds of 1500 and 2000 RPM. The inlet

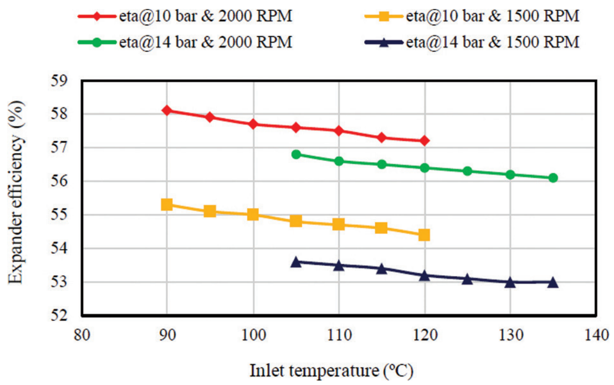

Figure 10. Effect of inlet temperature on expander efficiency.

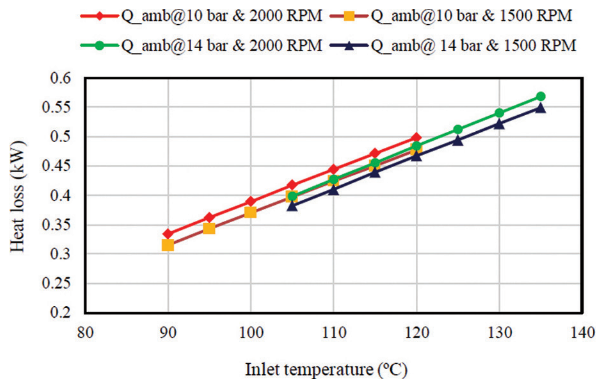

Figure 11. Effect of inlet temperature on heat loss to ambient.

temperature is varied from 90 to 120 °C at 10 bar and 105 to 135 °C at 14 bar. Fig.8 shows the trend of mass flow rate when inlet temperature (degree of superheat) is increased. It is seen that the mass flow rate of the working fluid decreases slightly, as the density of the fluid decreases. The mass flow rate is high in the case where inlet pressure is at 14 bar and shaft speed is at 2000 RPM.

From fig.9 it can be observed that the shaft power remains nearly constant when inlet temperature is increased. Therefore, it can be inferred that the enthalpy gain across the expander is nullified due to the decrease in the mass flow rate. Superheating does not benefit in increasing the power output from the expander. However, the degree of superheat of the fluid determines the quantum of heat exchange with the wall in the isobaric cooling process, modelled at the inlet. This thermal energy which is exchanged is an important component similar to the power loss. This will decide the amount of heat thatis vented out to the environment. Increasing inlet temperature beyond a certain limit increases the wall temperature. This leads to thermal energy dissipation. Thermal energy dissipation increases with inlet temperature for all curves as shown in fig. 11. This also leads to the deterioration in efficiency of the expander as shown in fig.10. The curves with higher shaft speeds dissipate more heat. Higher shaft speed increases the wall temperature, as high shaft speeds lead to more frictional power loss.

CONCLUSION

The present work focuses on the parametric investigation of the open-drive scroll expander used for micro-organic Rankine cycle. The analysis was carried out using a validated semi-empirical model. Effect of key parameters such as expansion ratio, shaft speed, and expander inlet temperature on power output and expander efficiency was evaluated for four different cases. The main findings are as follows:

- The shaft power increases with an increase in expansion ratio. However, when the expander is operated in a range far from its adapted expansion ratio, the efficiency of the scroll expander decreases. The adapted expansion ratio is a function of the built-in-volume ratio. Therefore, the expander efficiency drops when the constant volume expansion takes over, as it is less efficient than isentropic expansion.
- The efficiency of the scroll expander decreases at higher shaft speeds despite the increase in the mass flow rate of the working fluid. The effect of net losses due to friction and other mechanical losses is more prevalent at higher shaft speeds.
- Superheating does not benefit in increasing the power output from the expander as the increase in enthalpy of the fluid is nullified by the decrease in mass flow rate. In addition, increasing expander inlet temperature increases the heat losses towards the metal envelope. This leads to a decrease in expander efficiency as well as the overall thermodynamic efficiency. The inlet temperature must be maintained at saturation temperature corresponding to the expander inlet pressure for better performance.

The proposed model for the investigated expander could be used with other working fluids, in order to test the scroll expander behaviour for improving its performance. The challenge, however, lies in integrating this model with the whole organic Rankine cycle system. The requirements of high cycle thermal efficiency need high expansion ratios at which the expander's efficiency deteriorated as per this study. Hence, it is necessary to carry out further studies to explore expanders that operate at high expansion ratios (>5) as well as high isentropic efficiencies.

NOMENCLATURE

$\dot{m}$	Mass flow rate (kg s^{-1})
A	Area (m^2)
h	Specific enthalpy (J kg^{-1})

$\dot{Q}$	Heat transfer rate (W)
UA	Heat transfer coefficient (W K^{-1})
C	Specific heat (J kg^{-1} K^{-1})
P	Pressure (Pa)
T	Temperature (°C)
$r_{v,in}$	Built in volume ratio
N	Rotational speed (RPM)
v	Specific volume ($m^3 kg^{-1}$)
$\dot{W}$	Power (W)

Greek Symbols

ρ	Density (Kgm^{-3})
γ	Isentropic exponent
τ	Effectiveness
	Torque (N-m)

Subscripts

su	supply
p	constant pressure
nom	nominal
s	swept
w	envelope/wall
cr	critical
thr	throat
ex	exhaust
leak	leakage
ad	adapted
sh	shaft
in	internal
loss	losses
is	isentropic
amb	ambient

DATA AVAILABILITY STATEMENT

No new data were created in this study. The published publication includes all graphics collected or developed during the study.

CONFLICT OF INTEREST

The author declared no potential conflicts of interest with respect to the research, authorship, and/or publication of this article.

ETHICS

There are no ethical issues with the publication of this manuscript.

REFERENCES

[1] NITI Aayog, Government of India. A report on National Energy Policy 2017.

[2] Man Wang, Jiangfeng Wang, Yuzhu Zhao, Pan Zhao, Yiping Dai. Thermodynamic analysis and optimization of a solar-driven regenerative organic Rankine cycle (ORC) based on flat-plate solar collectors.Appl therm eng 2013; 50: 816–825.

[3] Pei Gang, Li Jing, Ji Jie. Analysis of low temperature solar thermal electric generation using regenerative Organic Rankine Cycle. Appl therm eng 2010; 30: 998-1004.

[4] Amir Ghasemi, Nasim Hashemian, Alireza Noorpoor, Parisa Heidarnejad. Exergy Based Optimization of a Biomass and Solar Fuelled CCHP Hybrid Seawater Desalination Plant. Journal of Thermal Engineering 2017; 3(1): 1034–1043.

[5] Usman Muhammad, Muhammad Imran, Dong Hyun Lee , Byung Sik Park. Design and experimental investigation of a 1 kW organic Rankine cycle system using R245fa as working fluid for low-grade waste heat recovery from steam.Energy Convers. Manag 2015; 103: 1089-1100.

[6] Seyedali Seyedkavoosi , Saeed Javan , Krishna Kota. Exergy-based optimization of an organic Rankine cycle (ORC) for waste heat recovery from an internal combustion engine (ICE).Appl therm eng 2017;126: 447–457.

[7] Ali Volkan Akkaya. Performance Analyzing of an Organic Rankine Cycle Under Different Ambient Conditions. Journal of Thermal Engineering 2017; 3(5): 1498–1504.

[8] Esra Özdemir, Muhsin Kilic. Thermodynamic Analysis of Basic and Regenerative Organic Rankine Cycles Using Dry Fluids from Waste Heat Recovery. Journal of Thermal Engineering 2018; 4(5): 2381–2393.

[9] İbrahim Kaya, Asım Sinan Karakurt, Yasin Üst. Investigation of Waste Heat Energy in a Marine Engine with Transcritical Organic Rankine Cycle. Journal of Thermal Engineering 2020; 6(3): 282–296.

[10] Turgay Koroglu, Oguz Salim Sogut. Advanced Exergy Analysis of an Organic Rankine Cycle Waste Heat Recovery System of a Marine Power Plant. Journal of Thermal Engineering 2017; 3(2): 1136–1148.

[11] Manoj Dixit, Akhilesh Arora, S.C. Kaushik. Energy and Exergy Analysis of a Waste Heat Driven Cycle for Triple Effect Refrigeration. Journal of Thermal Engineering 2016; 2(5): 954–961.

[12] Guoquan Qiu, Yingjuan Shao, Jinxing Li, Hao Liu, Saffa.B. Riffat. Experimental investigation of a biomass-fired ORC-based micro-CHP for domestic applications. Fuel 2012; 96: 374–382.

[13] Xinghua Liu, Yufeng Zhang, Jiang Shen. System performance optimization of ORC-based geo-plant with R245fa under different geothermal water inlet temperatures. Geothermics 2017; 66: 134–142.

[14] Ali Husnu Bademlioglu, Recep Yamankaradeniz, Omer Kaynakli.Exergy Analysis of the Organic Rankine Cycle Based on the Pinch Point Temperature Difference. Journal of Thermal Engineering 2019; 5(3): 157–165.
[15] Maurizio Cambi, Roberto Tascioni, Luca Cioccolanti, Enrico Bocci. Converting a commercial scroll compressor into an expander: experimental and analytical performance evaluation. 4th international seminar on ORC power systems, ORC2017, Milano, Italy, Energy Procedia2017; 129: 363–370.
[16] E. Oralli , Md. Ali Tarique, C. Zamfirescu and I. Dincer. A study on scroll compressor conversion into expander for Rankine cycles. International Journal of Low-Carbon Technologies 2011; 6: 200–206.
[17] Janette Hogerwaard, Ibrahim Dincer, Calin Zamfirescu. Analysis and assessment of a new organic Rankine based heat engine system with/without cogeneration. Energy 2013; 62: 300–310.
[18] Sylvain Quoilin , Vincent Lemort, Jean Lebrun. Experimental study and modeling of an Organic Rankine Cycle using scroll expander. Appl. Energy 2010; 87: 1260–1268.
[19] Jen-Chieh Chang , Tzu-Chen Hung ,Ya-Ling He , Wenping Zhang. Experimental study on low-temperature organic Rankine cycle utilizing scroll type expander. Appl. Energy 2015; 155: 150–159.
[20] Sébastien Declaye, Sylvain Quoilin, Ludovic Guillaume, Vincent Lemort. Experimental study on an open-drive scroll expander integrated into an ORC (Organic Rankine Cycle) system with R245fa as working fluid. Energy 2013; 55: 173–183.
[21] K. Qiu, M. Thomas, M. Douglas. Investigation of a scroll expander driven by compressed air and its potential applications to ORC. Appl therm eng 2018; 135: 109-115.
[22] Zhiwei Ma, Huashan Bao, Anthony Paul Roskilly. Dynamic modelling and experimental validation of scroll expander for small scale power generation system. Appl. Energy 2017; 186: 262–281.
[23] Pardeep Garg , G.M. Karthik , Prashant Kumar , Pramod Kumar. Development of a generic tool to design scroll expanders for ORC applications. Appl therm eng 2016; 109: 878–888.
[24] M. G. Sobamowo, A. A. Yinusa.Power Series -After treatment Technique for Nonlinear Cubic Duffing and Double-Well Duffing Oscillators. Journal of Computational applied mechanics 2017; 48(2): 297–306.
[25] S. J. Ojolo, A. A. Yinusa, S. O. Ismail.Modelling of Temperature Distribution in Orthogonal Machining using Finite Element Method', Proceedings of the 15th International Conference on Manufacturing Research, Incorporating the 32nd National Conference on Manufacturing Research, University of Greenwich, UK.September 5–7, 2017.
[26] M. G. Sobamowo, O. Adeleye, A. A. Yinusa. Analysis of convective-radiative porous fin with temperature-dependent internal heat Generation and magnetic field using Homotopy Perturbation method. Journal of Computational and Applied Mechanics 2017; 12(2): 127–145.
[27] M. G. Sobamowo, A. T. Akinshilo, A. A. Yinusa. Thermo-Magneto-Solutal Squeezing Flow of Nanofluid between Two Parallel Disks Embedded in a Porous Medium: Effects of Nanoparticle Geometry, Slip, and Temperature Jump Conditions. Hindawi Modelling and Simulation in Engineering 2018;Article ID 7364634.
[28] M. G. Sobamowo, A. A. Yinusa. Transient Combustion Analysis for Iron Micro-particles in a Gaseous Oxidizing Medium Using Adomian Decomposition Method. Journal of Computational Engineering and Physical Modeling 2018; 1: pp. 01–15.
[29] M. G. Sobamowo, A. A. Yinusa. Thermo-fluidic parameters effects on nonlinear vibration of fluid conveying nanotube resting on elastic foundations using Homotopy Perturbation method. Journal of Thermal Engineering 2018; 4(8): 2211–2233.
[30] M. G. Sobamowo, K. C. Alaribe, A. A. Yinusa. Homotopy perturbation method for analysis ofsqueezing axisymmetric flow of first-grade Fluid under the effects of slip and magnetic Field. Journal of Computational and Applied Mechanics 2018;13(1): 51–65.
[31] M. G. Sobamowo, A. A. Yinusa. Transient Combustion Analysis for Iron Micro -particles in a Gaseous Oxidizing Medium Using a New Iterative Method. J. Computational and Engineering Mathematics 2018; 5(3).
[32] M. G. Sobamowo, A. T. Akinshilo, A. A. Yinusa, A. Oluwatoyin. Nonlinear Slip Effects on Pipe Flow and Heat Transfer of Third Grade Fluid with Nonlinear Temperature-Dependent Viscosities and Internal Heat Generation. Software Engineering 2018; 6(3): 69–88.
[33] G. A. Oguntala, M. G. Sobamowo, A. A. Yinusa, R. Abd-Alhameed. Application of Approximate Analytical Technique Using the Homotopy Perturbation Method to Study the Inclination Effect on the Thermal Behavior of Porous Fin Heat Sink. J. Mathematical and Computational Applications 2018; 23(62), doi:10.3390/mca23040062.
[34] Sobamowo MG, Yinusa AA, Oluwo AA.Finite element analysis of flow and heat transfer of dissipative Casson-Carreau nanofluid over a stretching sheet embedded in a porous medium. Aeron Aero Open Access J. 2018; 2(5): 294–308.

[35] Sobamowo MG, Yinusa AA, Oluwo AA. Slip analysis of magnetohydrodynamics flow of an upper-convected Maxwell viscoelastic nanofluid in a permeable channel embedded in a porous medium', Aeron Aero Open Access J.2018; 2(5): 310–318.

[36] M. G. Sobamowo, G. A. Oguntala, A. A. Yinusa. On the Effects of Inclination Angle and Temperature-Dependent Internal Heat Generation on the Thermal Performance of Porous Fin Heat Sink.J Therm Sci Eng Appl 2018; 4(2): 34–47.

[37] M. G. Sobamowo, G. A. Oguntala, A. A. Yinusa. Nonlinear Transient Thermal Modeling and Analysis of a Convective-Radiative Fin with Functionally Graded Material in a Magnetic Environment. Hindawi, J. Model Simulat Eng 2019; Article ID 7878564.

[38] A. A. Yinusa, M. G. Sobamowo.Analysis of Dynamic Behaviour of a Tensioned Carbon Nanotube in Thermal and Pressurized Environments. Karbala International Journal of Modern Science 2019; 5(1): 1–11.

[39] A. A. Yinusa, M. G. Sobamowo. On The Transient Combustion Analysis for Iron Micro-particles in a Gaseous Oxidizing Medium Using Variational Iteration Method. J Reliab. Eng. Resil 2019; 1(1): 01–12.

[40] Davide Ziviani, Nelson A. James, Felipe A. Accorsi, James E. Braun, Eckhard A. Groll, Experimental and numerical analyses of a 5 kWe oil-free open-drive scroll expander for small-scale organic Rankine cycle (ORC) applications. Appl. Energy 2018; 230: 1140–1156.

[41] Jingye Yang, Ziyang Sun, Binbin Yu, Jiangping Chen. Modeling and optimization criteria of scroll expander integrated into organic Rankine cycle for comparison of R1233zd(E) as an alternative to R245fa. Appl therm eng 2018; 141: 386–393.

[42] Vincent Lemort, Sylvain Quoilin , Cristian Cuevas, Jean Lebrun. Testing and modeling a scroll expander integrated into an Organic Rankine Cycle.Appl therm eng 2009; 29: 3094–3102.

[43] Antonio Giuffrida. Modelling the performance of a scroll expander for small organic Rankine cycles when changing the working fluid. Appl therm eng 2014; 70: 1040–1049.

[44] Vincent Lemort, Declaye S, Quoilin S. Experimental characterization of a hermeticscroll expander for use in a micro-scale Rankine cycle.P I Mech Eng A-J Pow 2012; 226: 126–36.

[45] Wang, H., Peterson, R.B., Herron, T. Experimental performance of a compliant scroll expander for an organic Rankine cycle. P I Mech Eng A-J Pow 2009; 223(7): 863–872.